Journal of Current Research in Oral Surgery
2025, Volume 5, Issue 2, Page No: 147-155

Available online at: www.tsdp.net

ISSN: 3062-3480

Original Article

Positional Variability of the Mandibular Lingula among Distinct Ramus Morphologies: A CBCT Study

Andreas Müller[1]*, Stefan Weber[1], Julia Hoffmann[2], Lukas Schneider[1], Tobias Klein[2]

[1]Department of Oral Surgery and Dental Implantology, Faculty of Dentistry, Heidelberg University, Heidelberg, Germany.
[2]Department of Maxillofacial Clinical Research, Faculty of Medicine, Technical University of Munich, Munich, Germany.

***E-mail** ✉ andreas.mueller@gmail.com

Received: 04 June 2025; **Revised:** 10 October 2025; **Accepted:** 12 October 2025

ABSTRACT

When undertaking specific mandibular surgeries—such as sagittal split ramus osteotomy (SSRO) and intraoral vertical ramus osteotomy (IVRO)—the lingula provides an essential reference point. This research was designed to map lingula location along horizontal and vertical planes relative to four distinct ramus morphologies. A total of ninety subjects—60 female, 30 male—had cone beam computed tomography images reviewed to quantify the lingula tip (Li) in reference to the anterior border (AB), posterior border (PB), sigmoid notch (SN), and inferior border (IB) of the ramus. Proportional placement of Li on both axes was denoted by the indices Li–AB/AB–PB and Li–SN/SN–IB. Four lingula categories were recognized: triangular, truncated, nodular, and assimilated. Statistical testing was applied to evaluate measurement discrepancies across the four morphological groups and between the two sexes. On average, the Li–AB span measured 18.88 mm, a distance that proved substantially larger for the truncated configuration than for each of the other three variants. The Li–PB dimension averaged 15.23 mm, with no statistically significant difference among the four shapes. The computed Li–AB/AB–PB proportion reached 55.3% overall. For the truncated form, this value was 57.2%, significantly higher than the nodular form (54%) and the assimilated form (50.4%). The Li–SN distance averaged 19.95 mm, while Li–IB stood at 31.34 mm. Across the four lingula types, neither of these two measures varied significantly. The Li–SN/SN–IB ratio averaged 38.5%. Comparing the sexes revealed no significant differences in measurements. Substantial positional variation was evident among the four lingula forms, with Li situated superoposteriorly relative to the ramus midpoint. Acknowledging lingula shape heterogeneity is therefore imperative for the safe execution of ramal SSRO and IVRO interventions.

Keywords: Cone beam computerized tomography, Mandibular foramen, Lingula shape, Sagittal split ramus osteotomy, Intraoral vertical ramus osteotomy

How to Cite This Article: Müller A, Weber S, Hoffmann J, Schneider L, Klein T. Positional Variability of the Mandibular Lingula among Distinct Ramus Morphologies: A CBCT Study. J Curr Res Oral Surg. 2025;5(2):147-55. https://doi.org/10.51847/gCZZmofDHh

Introduction

Projecting from the internal face of the mandible, the mandibular lingula forms a tongue-like osseous crest above the mandibular foramen. Tuli *et al.* [1] delineated a four-category classification: triangular, truncated, nodular, and assimilated. Deriving from Meckel's cartilage [2], the sphenomandibular ligament (SML) constitutes a dense, flattened, and slender fibrous band. Its anchorage extends superiorly to the sphenoid spine and inferiorly across both the lingula and the mandibular foramen (MF) inferior rim. Through the MF, the inferior alveolar nerve (IAN) and corresponding vessels gain entry into the mandibular canal. Clinician awareness of lingula positioning vis-à-vis the mandibular foramen (MF) and inferior alveolar nerve (IAN) carries considerable importance. Enhanced anatomical knowledge in this area can

improve the success rate and procedural efficiency of IAN blockade for dental anesthesia, thereby refining treatment outcomes and adjunctive surgical maneuvers.

Surveying published morphological data on the mandibular lingula, Hsu *et al*. [3] documented that triangular anatomy prevailed across Indian cohorts, irrespective of sex. Among Thai and Brazilian groups, however, both males and females more commonly displayed the truncated type. Based on whether material comprised dry skeletal specimens or cone beam computed tomography (CBCT) scans, the triangular variant remained most prevalent in the dry mandible subset, with truncated, nodular, and assimilated patterns following in descending order. Yet, among CBCT images, the nodular category ranked first in frequency, followed by truncated, triangular, and assimilated forms. Sources of variation in the dry bone dataset might include age distribution, population ancestry, oral health status, and inherent osseous characteristics of the specimens, as well as the protocols employed for the acquisition and long-term storage of human mandibles. By contrast, while CBCT data bypass the artifacts associated with specimen preparation and preservation, interpretation of the resultant images can be compromised by diminished sharpness that occasionally occurs during digital reconstruction.

Two dominant techniques for the surgical correction of mandibular prognathism via mandibular setback are the sagittal split ramus osteotomy (SSRO) and the intraoral vertical ramus osteotomy (IVRO). Their procedural differences include the following: (1) In SSRO, the surgeon introduces purpose-designed instrumentation to gently reflect the medial soft tissue situated superiorly to the mandibular foramen, thereby protecting the inferior neurovascular bundle. A controlled split subsequently divides the ramus into medial and lateral osseous components. (2) For IVRO, the osteotomy line is drawn from the lateral aspect of the ramus and passes behind the lingula and MF. Division of the ramus yields distal and proximal fragments. The choice of surgical route depends heavily on the topographical relationships between the lingula and the mandibular foramen. An exhaustive grasp of these structural landmarks is essential for curtailing the potential of IAN and perivascular trauma intraoperatively; such injuries could lead to lasting sensory disturbance in the lower lip post-surgery [4]. Thus, a scrupulous evaluation of lingula configuration, coupled with accurate dimensional measurements, is a prerequisite for proficient SSRO and IVRO. The objective of this inquiry was to assess the horizontal and vertical ramal dimensions of four distinct lingula shapes and to detect any statistically significant discrepancies among them.

Materials and Methods

Acquisition of cone beam computed tomography imagery took place within the Density Department at Kaohsiung Medical University Chung-Ho Memorial Hospital. Scanning was conducted with each subject positioned in a natural head orientation and maintaining centric dental occlusion. Grounds for exclusion encompassed any of the following criteria: (1) craniofacial masses or disease processes, (2) inborn craniofacial malformations, or (3) a background of craniofacial trauma or operative procedures. The resulting CBCT DICOM files were transferred into RadiAnt DICOM Viewer version 4.6.9 (Medixant, Poznan, Poland) to render volumetric reconstructions. A suite of built-in measurement utilities provided by the software, including a linear ruler, was used to measure the distances under investigation. Serving as the horizontal plane of reference for the volumetric models **(Figure 1)** was the Frankfort horizontal plane, which is defined by a line connecting the lowermost point of the orbital cavity (Or: orbitale) and the uppermost aspect of the external acoustic opening (Po: porion). Following the scheme proposed by Tuli *et al*. [1], the lingula was grouped into four morphological variants: triangular, truncated, nodular, and assimilated **(Figure 2)**. As illustrated in **Figure 3**, metric acquisition relied on vertical and horizontal guidelines meeting at the apex of the lingula (Li). Along the horizontal axis, the following measurements were gathered: (1) Li–AB, corresponding to the interval separating Li from the anterior ramal margin; (2) Li–PB, representing the gap between Li and the posterior ramal margin; (3) AB–PB, the full breadth spanning the anterior and posterior ramal boundaries; and (4) the Li–AB/AB–PB quotient, which captures the relative anteroposterior placement of Li across the ramus. Along the vertical axis, the documented values included: (1) Li–SN, designating the span from Li to the sigmoid notch (SN); (2) Li–IB, the distance from Li downward to the inferior ramal border (IB); (3) SN–IB, the ramal height defined by the distance linking SN to IB; and (4) the Li–SN/SN–IB quotient, reflecting the relative superoinferior placement of Li between SN and IB.

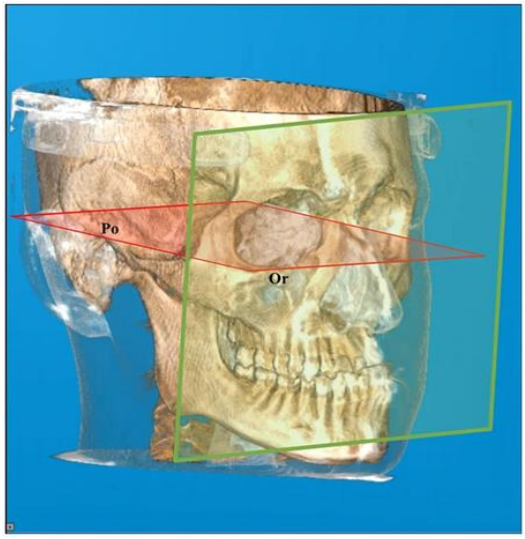

Figure 1. The Frankfort horizontal plane (red): a horizontal reference plane coursing between the inferior orbital rim (Or: orbitale) and the superior part of the external auditory meatus (Po: porion). Vertical plane (green): a vertical reference plane oriented at a right angle to the Frankfort horizontal plane.

a)

b)

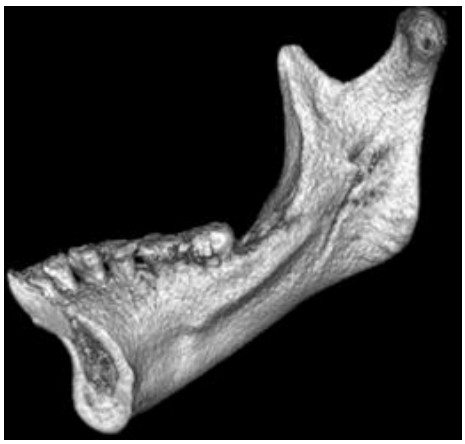

c)

d)

Figure 2. Four lingula variants were distinguished: (a) Triangular, (b) Truncated, (c) Nodular, and (d) Assimilated.

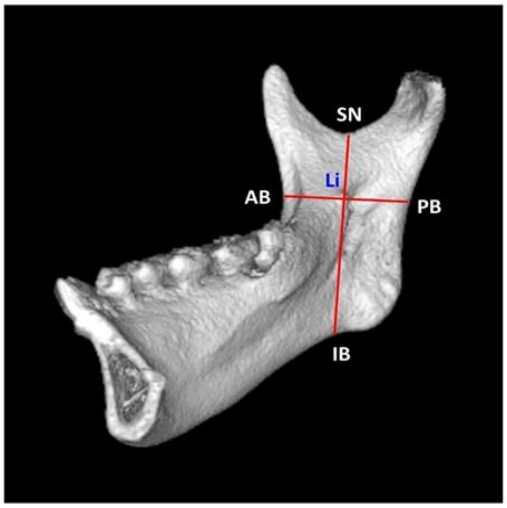

Figure 3. Distance readings and anatomical landmarks are projected onto the vertical and horizontal reference planes. Lingula tip (Li), anterior border of the ramus (AB), posterior border of the ramus (PB), sigmoid notch (SN), and inferior border of the ramus (IB).

Statistical computations were performed in IBM SPSS 20 (SPSS, Chicago, IL, USA) to probe distance-related differences tied to the four lingula morphologies. Comparisons across the four categories were executed via analysis of variance (ANOVA). When ANOVA detected statistically significant effects, the Scheffé post hoc procedure was used to isolate specific group differences. The threshold for statistical significance was set at $P < 0.05$. The study additionally juxtaposed results gathered from female and male subjects. Ethical clearance was granted by the institutional review board of Kaohsiung Medical University (IRB No. KMUH-IRB-20160066).

Results and Discussion

CBCT datasets from 90 individuals, totaling 180 sides, served as the basis for analysis in this investigation **(Table 1)**. The triangular variant appeared on 44 sides, truncated on 59 sides, nodular on 68 sides, and assimilated on 9 sides [5]. The study population comprised 60 women (120 sides) together with 30 men (60 sides). Among female subjects, the breakdown by side was as follows: triangular on 31 sides, truncated on 37 sides, nodular on 48 sides, and assimilated on 4 sides. Within the male subset, triangular was encountered on 13 sides, truncated on 22 sides, nodular on 20 sides, and assimilated on 5 sides.

Table 1. Horizontal distances (mm) and ratios of lingula shapes across the total sides.

Category	Subtype (n)	Li–AB / AB–PB Ratio	AB–PB SD	AB–PB mean	Li–PB SD	Li–PB mean	Li–AB SD	Li–AB mean
Morphological type	Triangular (44)	0.558	2.67	33.37	1.92	14.73	2.47	18.64
	Truncated (59)	0.572	3.55	35.53	2.26	15.23	2.59	20.30
	Nodular (68)	0.540	3.09	33.47	1.81	15.39	2.40	18.08
	Assimilated (9)	0.504	3.27	33.40	1.95	16.57	1.72	16.83
	Overall (180)	0.553	3.29	34.12	2.02	15.23	2.66	18.88
Between-group comparison		**Li–AB/AB–PB**		**AB–PB**	**Li–PB**		**Li–AB**	
P-value		< 0.001*		0.001*	0.071		< 0.001*	
Post hoc results		2 > 3, 4; 1 > 4		2 > 1, 3	NS		2 > 1, 3, 4	

n, number of sides; Li, lingula; AB, anterior border of ramus; PB, posterior border of ramus.
Lingula shape: 1, Triangular; 2, Truncated; 3, Nodular; 4, Assimilated.
Significant, $P < 0.05$; NS: Not Significant.

Across the entire study sample **(Table 1)**, the separation measured from Li to AB yielded an overall mean of 18.88 mm. When stratified by morphology, the averages were as follows: triangular, 18.64 mm; truncated, 20.30 mm; nodular, 18.08 mm; and assimilated, 16.83 mm. A key observation was that the truncated class returned a mean Li–AB value that proved statistically larger than each of the remaining three classes. For the Li–PB interval, the grand mean settled at 15.23 mm, and the four shape groups did not deviate from one another to any statistically appreciable extent. The mean AB–PB width of the total sample was 34.12 mm. Here, too, the truncated variety showed measurements significantly higher than those of the triangular and nodular varieties. As a proportion, Li–AB/AB–PB averaged 55.3% for all sides combined. Within the truncated subset, this proportion increased to a mean of 57.2%, a figure significantly higher than the 54% observed for the nodular subset and the 50.4% observed for the assimilated subset.

Shifting to the vertical plane **(Table 2)**, all participants combined produced a mean Li–SN span of 19.59 mm. The shape-specific breakdown gave 19.03 mm (triangular), 19.97 mm (truncated), 19.76 mm (nodular), and 18.61 mm (assimilated), none of which differed from one another in a statistically meaningful fashion. The mean Li–IB distance computed across the entire cohort was 31.34 mm, while the overall SN–IB ramal height averaged 50.94 mm. For both measures, comparisons among the four morphologies did not reach statistical significance. The overall Li–SN/SN–IB proportion stood at 38.5%. The truncated form (39.4%) achieved a ratio significantly higher than both the triangular form (37.3%) and the assimilated form (35.1%). In parallel, the nodular form's mean of 38.8% was also significantly elevated relative to the assimilated form.

Table 2. Vertical distances (mm) and ratios of lingula shapes in the total sides.

Category	Subgroup (n)	Li–SN/SN–IB Ratio	SN–IB SD	SN–IB mean	Li–IB SD	Li–IB mean	Li–SN SD	Li–SN mean
Shape classification	Triangular (44)	0.373	4.67	50.83	3.51	31.80	3.54	19.03
	Truncated (59)	0.394	4.88	50.73	4.07	30.76	2.90	19.97

	Nodular (68)	0.388	5.05	50.92	3.88	31.15	3.17	19.76
	Assimilated (9)	0.351	6.04	53.00	4.25	34.39	3.23	18.61
	Combined Total (180)	0.385	4.94	50.94	3.92	31.34	3.19	19.59
Inter-group analysis	**Li–SN / SN–IB**		**SN–IB**		**Li–IB**		**Li–SN**	
P-value	0.026*		0.641		0.058		0.357	
Post hoc findings	2 > 1, 4; 3 > 4		NS		NS		NS	

n, number of sides; Li, lingula; SN, sigmoid notch; IB, inferior border of ramus.
Lingula shape: 1, Triangular; 2, Truncated; 3, Nodular; 4, Assimilated.
Significant, P < 0.05; NS: Not Significant.

Restricting the analysis to female subjects **(Tables 3 and 4)**, the truncated shape's mean Li–AB distance (19.52 mm) exceeded, with statistical significance, those belonging to the nodular shape (18.12 mm) and the assimilated shape (16.15 mm). The Li–AB/AB–PB proportion attributable to the truncated configuration (56.9%) exceeded those for both the nodular (54.7%) and assimilated (50.1%) configurations. Additionally, the triangular configuration's mean ratio of 56.1% was significantly greater than that of the assimilated variant. Within the vertical dimension, no statistically meaningful variation emerged across the four shapes for the mean distances Li–SN, Li–IB, or SN–IB. Li–SN/SN–IB ratios were, however, significantly larger in the nodular (39.9%) and truncated (39.6%) shapes when each was contrasted with the assimilated shape (34.5%).

Table 3. Horizontal distances (mm) and ratios of lingula shapes in the females.

Category	**Subtype (n)**	**Li–AB/AB–PB ratio**	**AB–PB SD**	**AB–PB mean**	**Li–PB SD**	**Li–PB mean**	**Li–AB SD**	**Li–AB mean**
Shape groups	Triangular (31)	0.561	2.54	32.94	1.95	14.45	2.22	18.48
	Truncated (37)	0.569	3.06	34.36	2.26	14.84	2.35	19.52
	Nodular (48)	0.547	3.21	33.10	1.85	14.98	2.40	18.12
	Assimilated (4)	0.501	4.22	32.20	2.29	16.05	2.34	16.15
	Overall Sample (120)	0.556	3.06	33.42	2.02	14.84	2.43	18.58
Between-shape comparison		**Li–AB/AB–PB**			**AB–PB**	**Li–PB**		**Li–AB**
P-value		0.019*			0.143	0.424		0.009*
Post hoc results		2 > 3, 4; 1 > 4			NS	NS		2 > 3, 4

n, number of sides; Li, lingula; AB, anterior border of ramus; PB, posterior border of ramus.
Lingula shape: 1, Triangular; 2, Truncated; 3, Nodular; 4, Assimilated.
Significant, P < 0.05; NS: Not Significant.

Table 4. Vertical distances (mm) and ratios of lingula shapes in the females.

Category	**Subgroup (n)**	**Li–SN/SN–IB ratio**	**SN–IB SD**	**SN–IB mean**	**Li–IB SD**	**Li–IB mean**	**Li–SN SD**	**Li–SN mean**
Shape classification	Triangular (31)	0.379	4.75	50.34	3.44	31.20	3.30	19.14
	Truncated (37)	0.396	4.50	49.19	3.50	29.74	2.73	19.44
	Nodular (48)	0.399	5.26	49.92	3.54	29.96	3.30	19.96
	Assimilated (4)	0.345	1.53	48.40	0.82	31.68	1.51	16.73
	Overall (120)	0.391	4.80	49.75	3.47	30.27	3.12	19.48
Inter-group comparison		**Li–SN/SN–IB**		**SN–IB**		**Li–IB**	**Li–SN**	
P-value		0.043*		0.722		0.253	0.200	
Post hoc findings		2 > 4; 3 > 4		NS		NS	NS	

n, number of sides; Li, lingula; SN, sigmoid notch; IB, inferior border of ramus.
Lingula shape: 1, Triangular; 2, Truncated; 3, Nodular; 4, Assimilated.
Significant, P < 0.05; NS: Not Significant.

When the male subgroup was examined separately **(Tables 5 and 6)**, the truncated shape again stood out: its mean Li–AB measure of 21.62 mm was significantly higher than those for the triangular (19.02 mm), nodular (17.99 mm), and assimilated (17.38 mm) morphologies. The truncated ramus also possessed a mean AB–PB distance (37.50 mm) that significantly exceeded those of the triangular (34.42 mm) and nodular (34.35 mm) rami. The Li–AB/AB–PB ratio reached a mean of 57.7% for the truncated shape, a value significantly greater than the 55% observed for the triangular shape and the 52.2% for the nodular shape. In vertical terms, neither the average Li–SN, Li–IB, and SN–IB distances nor the mean Li–SN/SN–IB

proportion showed any significant inter-shape differences among males. Direct comparisons between female and male participants revealed no significant differences in any horizontal or vertical distance, the Li–AB/AB–PB proportion, or the Li–SN/SN–IB proportion.

Table 5. Horizontal distances (mm) and ratios of lingula shapes in the males.

Category	Subtype (n)	Li–AB/AB–PB Ratio	AB–PB SD	AB–PB Mean	Li–PB SD	Li–PB mean	Li–AB SD	Li–AB mean
Shape groups	Triangular (13)	0.550	2.79	34.42	1.74	15.40	3.04	19.02
	Truncated (22)	0.577	3.50	37.50	2.16	15.88	2.49	21.62
	Nodular (20)	0.522	2.65	34.35	1.32	16.37	2.45	17.99
	Assimilated (5)	0.507	2.34	34.36	1.79	16.98	0.99	17.38
	Overall Sample (60)	0.547	3.30	35.52	1.80	16.03	3.00	19.49
Between-shape analysis		**Li–AB / AB–PB**		**AB–PB**		**Li–PB**		**Li–AB**
P-value		0.001*		0.004*		0.287		< 0.001*
Post hoc results		2 > 3, 4		2 > 1, 3		NS		2 > 1, 3, 4

n, number of sides; Li, lingula; AB, anterior border of ramus; PB, posterior border of ramus.
Lingula shape: 1, Triangular; 2, Truncated; 3, Nodular; 4, Assimilated.
Significant, P < 0.05; NS: Not Significant.

Table 6. Vertical distances (mm) and ratios of lingula shapes in the males.

Category	Subgroup (n)	Li–SN/SN–IB ratio	SN–IB SD	SN–IB Mean	Li–IB SD	Li–IB mean	Li–SN SD	Li–SN mean
Shape categories	Triangular (13)	0.359	4.43	51.99	3.37	33.22	4.19	18.77
	Truncated (22)	0.392	4.45	53.33	4.45	32.48	3.02	20.85
	Nodular (20)	0.361	3.59	53.31	3.14	34.02	2.87	19.29
	Assimilated (5)	0.355	5.76	56.68	4.73	36.56	3.57	20.12
	Overall sample (60)	0.372	4.34	53.31	3.92	33.49	3.33	19.82
Between-shape comparison		**Li–SN/SN–IB**		**SN–IB**		**Li–IB**		**Li–SN**
P-value		0.174		0.241		0.175		0.271
Interpretation		NS		NS		NS		NS
Between-gender comparison		**Li–SN / SN–IB**		**SN–IB**		**Li–IB**		**Li–SN**
P-value		0.234		0.288		0.080		0.756
Interpretation		NS		NS		NS		NS

n, number of sides; Li, lingula; SN, sigmoid notch; IB, inferior border of ramus.
NS: Not Significant.

Operating within the confines of the lingula, mandibular foramen (MF), or mandibular canal of the ramus introduces a risk of trauma to the inferior alveolar neurovascular structures. The sequelae may include profuse surgical hemorrhage and postoperative anesthesia of the lower lip. It follows that the precise localization of the lingula, MF, and occlusal plane (OP), along with the metric relationships linking them, becomes critically important whenever ramus surgery is undertaken.

Span of Li to the anterior ramal border and to the posterior ramal border (Li–AB and Li–PB)

Several authors have based their investigations on osteological collections of dry mandibles [6-8]. In a Thai series, Jansisyanont *et al*. [6] arrived at a mean Li–AB measurement of 20.6 mm. A South Korean study by Park *et al*. [7] reported a mean of 18.89 mm, and a Brazilian study by Monnazzi *et al*. [8] reported a mean of 16.50 mm. An appreciable body of research has also drawn upon CBCT acquisitions from live subjects [9-11]. Sekerci and Sisman [9], studying Turkish individuals, quoted a mean Li–AB gap of 16.77 mm; Senel *et al*. [10], likewise in a Turkish group, reported 18.5 mm. Lupi *et al*. [11] furnished a mean of 16.96 mm for an Italian cohort. The figure emerging from our data was 18.88 mm. Such variation across the literature illustrates that ethnicity, together with the methodological distinction between direct osteometric readings and indirect CBCT-derived measurements, materially shapes the outcomes. Equally influential were the mandibular positioning protocols and the specific horizontal and vertical reference constructs adopted by each research team.

Among the overall sample, the assimilated class of lingula gave the shortest mean Li–AB value at 16.83 mm, whereas the truncated class yielded the longest at 20.30 mm. The truncated morphology's Li–AB

dimension surpassed, to a statistically significant degree, that of every other morphological category. A clinical implication is that the surgeon ought to approach the medial horizontal bone cut of an SSRO with extra caution when a truncated lingula is present. One should anticipate extending the osteotomy by an additional 3–4 mm beyond the length sufficient for an assimilated variant, to ensure reaching the Li. Preoperative planning with three-dimensional radiographic studies is indispensable for such cases. Additionally, our comparison of male and female data revealed no statistically significant differences in Li siting across the four lingula morphologies.

Turning to the Li–PB span and the Li–AB/AB–PB index, published means include the following: Jansisyanont *et al*. [6], 18 mm and a ratio of 53.2%; Park *et al*. [7], 18.89 mm and 55%; Monnazzi *et al*. [8], 14.63 mm and 53%; Sekerci and Sisman [9], 13.02 mm and 56%; Senel *et al*. [10], 16.9 mm and 53%; Lupi *et al*. [11], 15.28 mm and 53%. The current study's mean Li–PB distance was 15.23 mm, which did not differ significantly across lingula shapes. Li was positioned, on average, at 55% of the AB–PB breadth. The truncated configuration registered the highest Li–AB/AB–PB quotient (57%), in striking contrast to the assimilated configuration, which reached just 50%. Statistically significant ratio differences emerged among the four shape groups, confirming that lingula geometry directly governs anteroposterior Li placement within the ramus.

Span of SN to Li and IB to Li (SN–Li and IB–Li)

A mean SN–Li measure of 16.6 mm was reported by Jansisyanont *et al*. [6]. Lupi *et al*. [11] documented a mean SN–Li of 13.87 mm, a mean IB–Li of 31.2 mm, and a Li location corresponding to 31% of the total SN–IB dimension. Alves and Deana [12] recorded a mean SN–Li of 17.29 mm, a mean IB–Li of 33.3 mm, and Li at 34% of the SN–IB height. Senel *et al*. [10] supplied a mean SN–Li of 18.1 mm, a mean IB–Li of 38.3 mm, and Li at 32% of the SN–IB height. Our own series produced an average SN–Li of 19.59 mm and an average IB–Li of 31.34 mm. Neither of these two linear measures differed significantly across the four lingula configurations. The Li lay at 38.5% of the SN–IB interval. Differences in this proportional value among the shapes were statistically significant: the nodular (39.9%) and truncated (39.6%) types both posted Li–SN/SN–IB ratios that were notably higher than that recorded for the assimilated type (34.5%).

What our findings underscore is that lingula morphology carries genuine weight in dictating superior-inferior Li positioning. Earlier works [6, 10-12] have cataloged shifts in linear lingula coordinates driven by ethnic background, age, sex, anatomical reference frameworks, and landmark selection criteria. The proportional relationship SN–Li to SN–IB, however, appeared to exhibit only modest fluctuation between dry mandible data and CBCT data. One limitation of the present study is the absence of side-by-side analysis. We therefore cannot comment on whether bilateral differences exist at the individual level or across the aggregate sample. A future objective is to determine whether the averaged distances and ratios are symmetrical between the right and left sides, or whether asymmetries are detectable.

When planning an SSRO, the surgeon must weigh not only the Li and MF dimensions but also the lingula's height. Alves and Deana [12], working with Brazilian Caucasians, reported a mean lingual height of 8.89 mm in males and 7 mm in females. Zhou *et al*. [13] gave corresponding figures for a Korean adult population: 10.1 mm (males) and 9.8 mm (females), with inter-sex differences failing to reach significance. In a Taiwanese context, Hsu *et al*. [14] found that male lingual height averaged 8.73 mm, which was significantly greater than the female average of 7.76 mm. Concerning the lingula's vertical relationship to the occlusal plane, Jansisyanont *et al*. [6] observed that 80% of lingulae resided 4.5 mm above the plane. Zhou *et al*. [13] noted that a lingula positioned inferior to the occlusal plane is an uncommon finding; most were sited roughly 5.9 ± 3.0 mm superior to it. Akcay *et al*. [15] further demonstrated, in Turkish subjects, that the Class III measurement (mean 9.91 mm) was significantly greater than that for Class I individuals (mean 8.12 mm).

Beyond this, assessment of the cortical and cancellous bone stock occupying the interval between SN and Li is necessary, along with evaluation of the junctional zone where the medial and lateral cortices become confluent. Where cancellous bone proves meager in thickness, the act of performing a medial horizontal osteotomy intended to cleave the medial from the lateral ramal segment during SSRO can amplify the danger of outer-cortex fracturing and a resultant unfavorable split. Such a risk persists irrespective of whether the bony cut engages the external cortex directly. According to Smith *et al*. [16], the vertical distance from Li to the point of cortical coalescence ranged from 7.5 to 13.3 mm. The authors counseled that the medial horizontal osteotomy line should be placed either exactly at or fractionally above the Li plane. They also underscored that a more superiorly sited osteotomy could compound the technical difficulty of splitting the bone or magnify the chance of

sustaining an adverse fracture pattern. Tom *et al*. [17] established that extending a medial horizontal osteotomy upward by greater than 5 mm from Li raises the probability of transecting the region where the medial and lateral cortical plates merge. Suzen *et al*. [18] probed the bearing that medial horizontal osteotomy placement has upon postoperative complications and neurosensory disturbance. Their results revealed that osteotomies executed superior to Li were accompanied by considerably diminished complication rates and sensory deficits when set against those placed in an inferior location. Confining the osteotomy to the vicinity of Li itself, a zone where an ample width of cancellous bone is retained, can lessen the likelihood of a cleavage occurring exclusively in cortical bone.

Measurements reported by Jansisyanont *et al*. [6] indicated a mean breadth at the MF of 4.7 mm, with values ranging from 2.9 to 6.8 mm. Park *et al*. [7] recorded distances from the MF's posterior boundary to AB and PB as 19.69 mm and 14.41 mm, respectively, and noted that the posterior edge of the MF was positioned at approximately 58% along the anteroposterior axis and 46% along the superoinferior axis of the ramus. Apinhasmit *et al*. [19] documented corresponding separations of 22.3 mm to AB and 12.7 mm to PB, situating the MF posterior edge at roughly 64% of the ramal anteroposterior dimension. Collectively, these data confirm that the MF's posterior border resides predominantly behind the lingula. Grasping the spatial coordinates of both Li and MF is vital for the safe execution of operations such as SSRO and IVRO. In the context of SSRO, Wolford [20] advocated that the medial horizontal osteotomy be carried out superior to Li and directed toward the region posterior to both Li and the MF. Muto *et al*. [21] examined cancellous bone architecture after medial horizontal osteotomy application during SSRO. They observed that subjects with Class III skeletal relationships had a thinner, more irregularly contoured, and less uniformly distributed cancellous layer, with these features particularly pronounced anterior and posterior to the MF. On this basis, they identified the most favorable and secure site for the medial horizontal osteotomy as immediately above Li, with a modest posterior extension of 5 to 6 mm.

To carry out an SSRO effectively, the lingula's position in relation to the occlusal plane must be ascertained from radiographic images. A cautious and precise operative technique is paramount to prevent inadvertent damage to either the lingula or the MF; such trauma carries the potential for profuse intraoperative hemorrhage and, in the postoperative period, sensory loss affecting the lower lip. During the medial horizontal osteotomy phase of SSRO, there is no obligation to locate the lingula by sight or by palpation. We therefore endorse performing the osteotomy at least 5 mm above the occlusal plane to reduce the risk of injury to the IAN and its accompanying vascular structures.

Conclusion

The present work revealed pronounced positional heterogeneity among the four lingula configurations. Statistically meaningful disparities were detected in Li siting along both horizontal and vertical axes, along with significant differences in the Li–AB/AB–PB and Li–SN/SN–IB proportional values. The average Li–AB dimension recorded for the truncated morphology was significantly larger than the corresponding means for the other three morphologies. Accordingly, heightened attention to lingula shape diversity and to the associated spatial measurements is indispensable when undertaking SSRO and IVRO on the mandibular ramus.

Acknowledgments: None

Conflict of Interest: None

Financial Support: None

Ethics Statement: The study was approved by the Institutional Review Board of Kaohsiung Medical University (IRB No. KMUH-IRB-20160066).

References

1. Tuli A, Choudhry R, Choudhry S, Raheja S, Agarwal S. Variation in shape of the lingula in the adult human mandible. J Anat. 2000;197:313-7. doi:10.1046/j.1469-7580.2000.19720313.x
2. Rodríguez Vázquez JF, Mérida Velasco JR, Jiménez Collado J. Development of the human sphenomandibular ligament. Anat Rec. 1992;233:453-60. doi:10.1002/ar.1092330312
3. Hsu KJ, Lee HN, Chen CM. Morphological investigation of mandibular lingula: a literature review. J Pers Med. 2022;12:1015. doi:10.3390/jpm12061015
4. Colella G, Cannavale R, Vicidomini A, Lanza A. Neurosensory disturbance of the inferior alveolar nerve after bilateral sagittal split osteotomy: a systematic review. J Oral Maxillofac Surg. 2007;65:1707-15. doi:10.1016/j.joms.2007.05.009

5. Chen CM, Lee HN, Liang SW, Hsu KJ. Morphological study of the mandibular lingula and antilingula by cone-beam computed tomography. Bioengineering. 2023;10:170. doi:10.3390/bioengineering10020170
6. Jansisyanont P, Apinhasmit W, Chompoopong S. Shape, height, and location of the lingula for sagittal ramus osteotomy in Thais. Clin Anat. 2009;22:787-93. doi:10.1002/ca.20849
7. Park JH, Jung HD, Kim HJ, Jung YS. Anatomical study of the location of the antilingula, lingula, and mandibular foramen for vertical ramus osteotomy. Maxillofac Plast Reconstr Surg. 2018;40(1):15. doi:10.1186/s40902-018-0155-3
8. Monnazzi MS, Passeri LA, Gabrielli MF, Bolini PD, de Carvalho WR, da Costa Machado H. Anatomic study of the mandibular foramen, lingula and antilingula in dry mandibles, and its statistical relationship between the true lingula and the antilingula. Int J Oral Maxillofac Surg. 2012;41:74-8. doi:10.1016/j.ijom.2011.08.009
9. Sekerci AE, Sisman Y. Cone-beam computed tomography analysis of the shape, height, and location of the mandibular lingula. Surg Radiol Anat. 2014;36:155-62. doi:10.1007/s00276-013-1150-0
10. Senel B, Ozkan A, Altug HA. Morphological evaluation of the mandibular lingula using cone-beam computed tomography. Folia Morphol. 2015;74:497-502. doi:10.5603/FM.2015.0114
11. Lupi SM, Landini J, Olivieri G, Todaro C, Scribante A, Rodriguez Y, et al. Correlation between the mandibular lingula position and some anatomical landmarks in cone beam CT. Healthcare. 2021;9:1747. doi:10.3390/healthcare9121747
12. Alves N, Deana NF. Morphological study of the lingula in adult human mandibles of Brazilians individuals and clinical implications. Biomed Res Int. 2015;2015:873751. doi:10.1155/2015/873751
13. Zhou C, Jeon TH, Jun SH, Kwon JJ. Evaluation of mandibular lingula and foramen location using 3-dimensional mandible models reconstructed by cone-beam computed tomography. Maxillofac Plast Reconstr Surg. 2017;39:30. doi:10.1186/s40902-017-0128-y
14. Hsu KJ, Tseng YC, Liang SW, Hsiao SY, Chen CM. Dimension and location of the mandibular Lingula: comparisons of gender and skeletal patterns using cone-beam computed tomography. Biomed Res Int. 2020;2020:2571534. doi:10.1155/2020/2571534
15. Akcay H, Kalabalık F, Tatar B, Ulu M. Location of the mandibular lingula: comparison of skeletal class I and class III patients in relation to ramus osteotomy using cone-beam computed tomography. J Stomatol Oral Maxillofac Surg. 2019;120:504-8. doi:10.1016/j.jormas.2019.07.013
16. Smith BR, Rajchel JL, Waite DE, Read L. Mandibular ramus anatomy as it relates to the medial osteotomy of the sagittal split ramus osteotomy. J Oral Maxillofac Surg. 1991;49:112-6. doi:10.1016/0278-2391(91)90095-4
17. Tom WK, Martone CH, Mintz SMA. Study of mandibular ramus anatomy and its significance to sagittal split osteotomy. Int J Oral Maxillofac Surg. 1997;26:176-8. doi:10.1016/S0901-5027(97)80814-4
18. Suzen M, Uckan S, Munevveroglu S, Ozel A. Effect of horizontal osteotomy level on complication rates and neurosensory deficits after sagittal split ramus osteotomy. J Craniofac Surg. 2021;32:1712-5. doi:10.1097/SCS.0000000000007404
19. Apinhasmit W, Chompoopong S, Jansisyanont P. Alternative landmarks of the mandibular foramen to prevent nerve injury during ramus surgery. J Med Assoc Thai. 2015;98:574-81.
20. Wolford LM. Influence of osteotomy design on bilateral mandibular ramus sagittal split osteotomy. J Oral Maxillofac Surg. 2015;73:1994-2004. doi:10.1016/j.joms.2015.03.023
21. Muto T, Shigeo K, Yamamoto K, Kawakami J. Computed tomography morphology of the mandibular ramus in prognathism: effect on the medial osteotomy of the sagittal split ramus osteotomy. J Oral Maxillofac Surg. 2003;61:89-93. doi:10.1053/joms.2003.50014